Magnesium Technology 2012
Edited by: Suveen N. Mathaudhu, Wim H. Sillekens, Neale R. Neelameggham, and Norbert Hort
TMS (The Minerals, Metals & Materials Society), 2012

Evaluating the effect of pre-ageing deformation on β' precipitate size and distribution in Mg-Zn(-Y) Alloys

Julian M Rosalie[1], Hidetoshi Somekawa[1], Alok Singh[1], Toshiji Mukai[2].

[1]Microstructure Design Group, National Institute for Materials Science (NIMS), Sengen 1-2-1, Tsukuba, Ibaraki, 305-0047, Japan.
[2]Dept. Mechanical Engineering, Kobe University, 1-1 Rokkodai, Nada, Kobe city, 657-8501 Japan.

Keywords: Magnesium alloys, Precipitation

Abstract

The effect of pre-ageing deformation on the precipitate diameter and length distribution in Mg-Zn(-Y) alloys was examined. Extrusion and pre-ageing deformation were used to introduce dislocations while precluding twin formation. Dislocations provided nucleation sites for rod-like β_1' precipitates, resulting in a refinement of the precipitate size distribution. In the binary alloy 5% strain reduced the average precipitate length from approximately 450nm to 60nm, and average diameter from 14 to 9 nm. Substantial reductions in precipitate size were also observed in the Mg-Zn(-Y) alloy. The average interparticle spacing of the rod-like precipitates was measured by Delaunay triangulation. The precipitate distribution was found to be significantly inhomogeneous, with measured interparticle spacings approximately 32% greater than predicted. For 5% pre-ageing deformation the yield strength of the binary alloy approached 95% of the ultimate tensile strength.

Introduction

Magnesium-zinc based alloys show a particularly strong age-hardening response compared to other commercial magnesium alloys [1]. The precipitate providing the greatest resistance to basal slip in these alloys is termed β_1' and takes the form of high aspect-ratio rods with $\langle 0001 \rangle$ habit [1].

Pre-ageing deformation of binary Mg-Zn alloys has been shown to accelerate the ageing process and increase the maximum hardness obtainable [2]. Reports of the precipitation of the β_1' precipitate on dislocations indicate that these defects are the primary nucleation sites [1, 3, 4]. While it has been shown that the hardness increment in response to cold-rolling reaches a plateau [2], the extent to which the precipitate size and diameter distribution can be refined by deformation has not been established.

In recent years there has been considerable interest in the judicious use of rare-earth elements and yttrium in magnesium alloys, particularly to improve high temperature properties such as creep resistance. Yttrium is poorly soluble in Mg [5] and generally partitions to Mg-Zn-Y ternary phase precipitates at the grain boundaries [3, 6, 7]. Although precipitation of the β_1' phase is not directly influenced by yttrium, the formation of the grain boundaries phases may affect the availability of zinc in the matrix and thus the extent and refinement of the β_1' precipitate distribution. Despite the interest in yttrium-bearing Mg-Zn based alloys there has been no yet been any attempt made to quantify how the presence of yttrium impacts on the distribution of the β_1' phase.

Nucleation on heterogeneous sites such as dislocations in magnesium alloys may also result in significant localisation of precipitation. It has been shown that that in nickel-based alloys clustering of dispersoids results in a highly inhomogeneous distribution [8] whose interparticle spacing is not well represented by standard stereological formulae. Several methods such as the used of Voronoi tessellation [8] and Delaunay triangulation [9] have been suggested to account for this difficulty. While Delaunay triangulation has been used to calculate more physically representative oxide dispersoid spacings in nickel-based alloys [9] to our knowledge it has not been applied to heterogeneous precipitation in magnesium alloys.

The present work has measured the β_1' precipitation length and diameter as a function of tensile pre-ageing deformation and the corresponding effect on the yield strength and ultimate tensile strength of the alloys. The interparticle spacing was measured directly via Delaunay triangulation to determine whether dislocations introduced via pre-ageing deformation lead to an inhomogeneous precipitate distribution.

Experimental

Billets of binary Mg-3.0at.%Zn and ternary Mg-3.0at.%Zn-0.5at.%Y alloys (hereafter designated 3000Z and 3005ZY, respectively) were prepared by directchill casting. The compositions were confirmed via inductively-coupled plasma mass spectroscopy (ICP-MS). Each billet was homogenised under a CO_2 atmosphere for 15 h at 300°C and 350°C, respectively for the binary and the ternary alloy. The homogenised billets were then extruded into 12 mm diameter rods at an extrusion ratio of 12:1 and temperatures of 300°C. Tensile samples of gauge length 15 mm and diameter 3 mm were machined from the extruded rods. These were encapsulated in helium and solution treated for 1 h at 300°C for alloy 3000Z and 400°C for alloy 3005ZY, and quenched into water.

Pre-ageing deformation was carried out using an Instron mechanical tester. Tensile deformation was applied parallel to the extrusion axis at a strain rate of $1 \times 10^{-3}\,s^{-1}$. Samples were deformed to a nominal plastic strain of either 3% or 5% in tension. Ageing was conducted in an oil bath at 150°C with the ageing response measured using Vickers hardness testing. Further tensile tests were then carried out in the Instron mechanical tester, at strain rates of $1 \times 10^{-3}\,s^{-1}$ on samples aged to peak hardness to determine yield strength and ultimate tensile strength.

Samples for TEM analysis were prepared from the aged specimens by first grinding to ~60 – 70 μm then polishing to perforation using a Gatan precision ion polishing system. TEM observations were conducted using a JEOL 4000EX instrument operating at 400 kV. Stereological measurements were carried out on scanned negatives using ImageJ software version 1.44. The cross-sectional areas of individual precipitates were directly determined from the images recorded along [0001] zone axis of the matrix grains by the analysis software (ImageJ). The area of individual precipitates was determined by using image processing software. Precipitate diameters were taken as the diameter for a cylindrical rod of equivalent area. The average centre-centre distance between β_1' particles was determined by Delaunay triangulation, using the Delaunay Voronoi plug-in for ImageJ (version 1.44). The mean interparticle spacing was determined by subtracting the mean precipitate diameter from the mean centre-centre distance determined by Delaunay triangulation.

Results

Pre-ageing deformation acted to significantly refine the diameter of the β_1' precipitates from 14 nm to 9 nm in the binary alloy and 19 nm to 11 nm in the ternary alloy. Figure 1 shows the decrease of the average diameter for Mg-Zn and Mg-Zn-Y alloys plotted against the plastic deformation applied before ageing. The error bars indicate the standard deviation the precipitate diameter and are not a measure of uncertainty of the average diameter. The lines are intended as a guide for the eye only and to indicate the monotonic decrease in precipitate diameter with increasing pre-ageing strain. The precipitate diameter in the ternary alloy was greater than that of binary Mg-Zn for approximately equivalent deformation, particularly in the non-deformed samples.

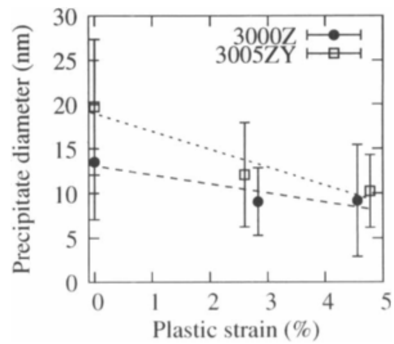

Figure 1: The average β_1' precipitate diameter in 3000Z and 3005ZY alloys as a function of pre-ageing strain. The lines are intended as a guide for the eye only. The precipitate diameter in the ternary alloy was greater than that of binary Mg-Zn for approximately equivalent deformation.

The precipitate length was also substantially reduced in samples subjected to pre-ageing deformation. Figure 2 shows the average precipitate length of the β_1' rods as a function of the plastic strain applied before ageing. In both alloys the average precipitate length drops substantially after 3% nominal strain, with a much more modest decrease between 3% and 5% nominal strain. Unlike the case of the precipitate diameter, there was little difference between the length values of precipitates in the binary and ternary alloys.

β_1' precipitate size and spacing

The average interparticle spacing, λ, was calculated using the stereological formula for cylindrical rods normal to the (0001) plane in Mg (Equation 1 [10]).

$$\lambda = \left(\frac{0.953}{\sqrt{f}} - 1 \right) d_1 \tag{1}$$

where f was the volume fraction and d_1 was the average precipitate diameter.

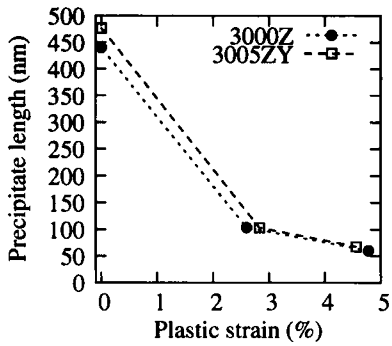

Figure 2: The average β_1' precipitate length in 3000Z and 3005ZY alloys as a function of pre-ageing strain. The lines are intended as a guide for the eye only.

This value was compared with average spacings determined by Delaunay triangulation of the images [9, 11]. Figures 3 and 4 present representative images showing β_1' precipitates with the triangulation overlaid on the micrograph. Visual inspection is sufficient to show that the precipitates are inhomogeneously distributed, with a tendency to lie along particular lines. In Figure 3(a) it can be clearly seen that such lines correspond to strain contrast indicating the location of dislocations. This resulted in a wide spread of near-neighbour particle spacings, with the particles in a given line being closely spaced, with considerably wider spacings between groups.

The measured and calculated particle spacings are compared in Figure 5. The dashed lines indicate the best fit through the Delaunay triangulation data, while the solid line indicates a homogeneous distribution. The error bars in the measured data indicate the standard error based on the spread in the particle spacing and the uncertainty in the volume fraction. While there is considerable spread in the data, the measured values are consistently greater than for a homogeneous distribution, with the gradient of the dashed line suggesting a discrepancy of approximately 32%. This is true even for the extreme case of the 3005ZY alloy in the non-deformed condition where the measured spacing was 277 nm or an order of magnitude greater than the 5% strained samples.

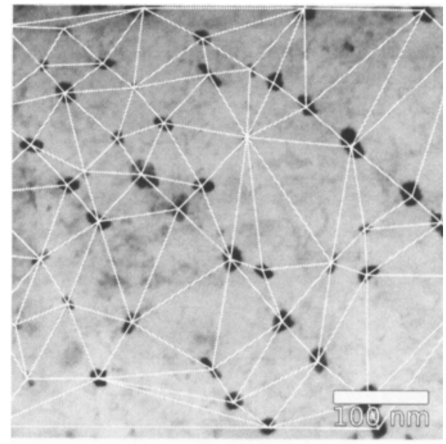

(a) 3000Z, 0% strain

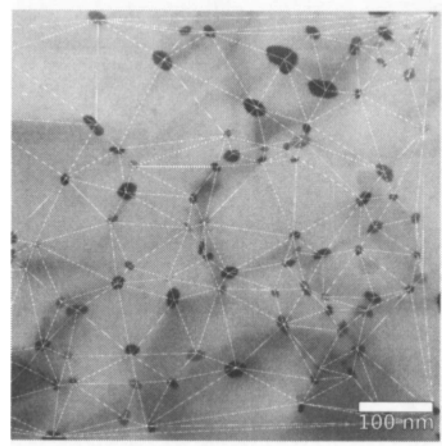

(b) 3000Z, 3% strain

Figure 3: Delaunay triangulations of electron micrographs of β_1' precipitates in 3000Z alloys.

Yield strength & ultimate tensile strength

The initial condition of the two alloys was similar, with yield strengths in the solution treated condition (143 ± 5 and 149 ± 1 MPa, respectively) as shown in Figure 6. However, after isothermal ageing (with or without deformation) the 3000Z alloy displayed greater strength than the 3005ZY alloy for identical treatment conditions. Ageing to optimum hardness resulted in substantial increases in the strength of the alloys, due to precipitation hardening, with the binary 3000Z alloys showing a more significant yield strength increment (273 ± 1 MPa) compared to the ternary alloy (218 ± 3 MPa). The application of pre-ageing deformation resulted in further increases in the yield strength which reached 309 ± 5 for the 3000Z alloy and 308 ± 5 MP for the 3005ZY alloy. The ultimate tensile strength of the 3000Z alloy displayed a gradual increase

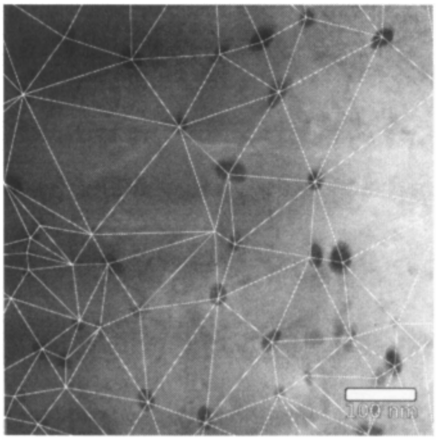

(a) 3005ZY, 3% strain

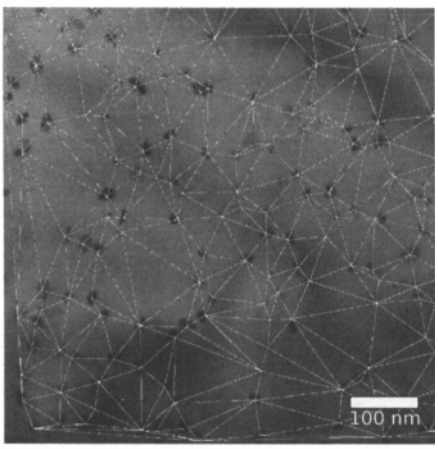

(b) 3005ZY, 5% strain

Figure 4: Delaunay triangulations of electron micrographs showing β_1' rod-shaped precipitates in 3005ZY.

with increasing pre-ageing deformation (281→322 MPa), however, in terms of true strain of the failure strain of 3000Z was virtually unchanged with and average value of 335MPa and a standard deviation of 2 MPa. The 3005ZY alloy showed a overall similar response, except that the sample aged without deformation showed markedly lower tensile strength. In the 3000Z alloys deformed either 3 or 5% before ageing, the yield strength is approximately 95% of the tensile strength and little further improvement in yield strength through pre-ageing deformation is to be expected.

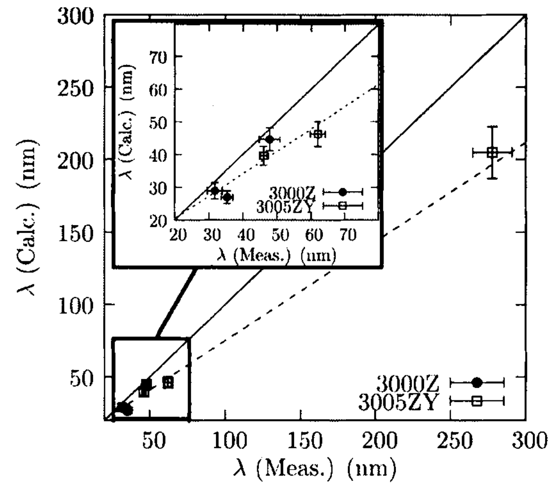

Figure 5: Measured vs calculated interparticle spacings (λ). Particle spacings measured directly from micrographs using Delaunay triangulation (See Figures 3 & 4). were significantly greater than those calculated assuming a homogeneous precipitate distribution. The dashed lines indicate the best fit through the measured points, while the solid line a homogeneous distribution i.e. equal measured and calculated values.

Discussion

The application of up to 5% pre-ageing deformation had a significant effect on the size and spacing of the β_1' precipitates and a subsequent improvement in the resistance to plastic deformation. The precipitate diameter and length did not appear to show the same behaviour as a function of plastic strain. Precipitate lengths in the binary and ternary alloys showed similar changes as a function of pre-ageing deformation, with a rapid decrease in length for 3% deformation with a slight further decrease after 5% pre-ageing deformation. In addition, for a given heat treatment condition there was ≤11% difference in the precipitate length, suggesting similar lengthening behaviour in the two alloys.

Precipitate diameter showed an approximately linear reduction with increasing pre-ageing plastic strain (Fig 1). There were substantially greater differences in the precipitate diameter between binary and ternary alloys, although as the diameter of precipitates in the ternary alloy decreasing more rapidly the values tended to converge. It should be noted that the graph shows only the plastic

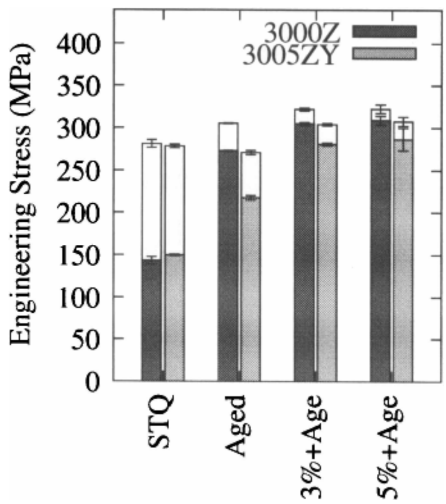

Figure 6: Alloy strength as a function of heat treatment. Filled and empty boxes show the yield and tensile strength of the alloys as a function of heat treatment condition. ("STQ" indicates the solution treated and quenched condition.)

strain (i.e. strain up to the yield point was neglected). Since twinning is negligible, increases in the plastic strain and should be in proportion with the extent of slip and hence (in very rough terms) with the dislocation density.

The difference in the lengthening and thickening response of the precipitates to deformation was thought to reflect competition between precipitate nucleation and precipitate growth. In non-deformed alloys the relatively few precipitate nuclei formed face little competition for solute and are able to grow extensively. Since lengthening of the rods is easier than lateral growth, such precipitates can reach extreme lengths (~450 nm in the case of the Mg-Zn-Y alloy). When heterogeneous sites such as dislocations are introduced, the number of nuclei is dramatically increased. These nuclei will lengthen and thicken – with growth primarily through lengthening – however they will face greater competition from one another and their growth will ultimately be restricted by the available solute.

For alloys in the peak-aged condition, it is generally considered that all available solute will be partitioned to the precipitates and the volume fraction of precipitates should be a function of the overall composition. In this case, then the above reasoning indicates that dispersion strengthening for rod-like precipitates normal to the Mg basal plane may best be improved by multiplying the number of available nuclei and restricting the their lengthening.

The inhomogeneity of the precipitate spacing is expected to have a significant effect on the effectiveness of precipitate strengthening. As shown in Figure 5 the measured interparticle particle spacings averaged roughly 32% more than would be expected for a homogeneous distribution. The Delaunay triangulation technique takes into account the variation in the precipitate spacing in this non-homogeneous system, which produces large non-strengthened regions of the matrix.

It was notable that although increasing deformation substantially refined the precipitate spacing, even for 5% tensile deformation, the measured precipitate spacing exceeded the expected value for a homogeneous system. This suggests that while the introduction of additional dislocations refines the precipitate distribution, it is does not help to overcome the inherent problem with heterogeneous nucleation; namely that precipitation will be concentrated at the defect sites.

Pre-ageing deformation was effective in supplementing the resistance of the alloys to plastic deformation compared to ageing without deformation. The binary alloy displayed greater improvements in yield strength than the ternary alloy, in accordance with the more refined precipitate distribution that was apparent from the the stereological measurements. Using 5% pre-ageing strain it was possible to achieve yield strengths up to 95% (3000Z) or 91% (3005ZY) of the ultimate tensile strength.

The isothermal ageing temperature of 150°C was sufficient for stress relief [12] and it is probable that during the early stages of ageing there is competition between nucleation of β_1' particles on dislocations and the loss of dislocations through annealing. This was consistent with the observation that most of the increase in yield strength occurred in the first 3% plastic deformation. The narrow window between yield strength and UTS, along with the diminishing rate of return for deformation suggests that tensile deformation beyond 5% is unlikely to further enhance the yield strength, particularly for Mg-Zn.

Conclusions

Pre-ageing tensile deformation up to 5% strain had a strong refining effect on the diameter and length of β_1' precipitates in Mg-Zn and Mg-Zn-Y alloys. The precipitates were distributed along dislocations in the matrix giving rise to a somewhat inhomogeneous precipitate distribution. Measurements of the interparticle spacing via

Delaunay triangulation were 32% greater than calculated values assuming a homogeneous precipitate distribution. Precipitation in the binary alloy was more responsive to pre-ageing deformation than in the ternary alloy and the binary alloy showed a greater increment in yield stress after pre-ageing deformation. Yield strengths in the binary alloy approached 95% of the ultimate tensile strength, suggesting that more extensive deformation would not greatly improve the resistance to plastic deformation.

References

[1] J. B. Clark, *Acta Metall.*, **13**:(1965) 1281.

[2] G. Mima, Y. Tanaka, *Trans Japan Inst Met*, **12**(2):(1971) 76.

[3] A. Singh, A. P. Tsai, *Scr. Mat.*, **57**:(2007) 941. doi: 10.1016/j.scriptamat.2007.07.028.

[4] K. Oh-ishi, K. Hono, *et al.*, *Mater Sci Eng*, **A 496**:(2008) 425. doi: 10.1016/j.msea.2008.06.005.

[5] H. Okamoto, *J Phase Equil*, **15**(1):(1994) 129. doi: 10.1007/BF02667700.

[6] L. Y. Wei, G. L. Dunlop, *et al.*, *Metall. Mater. Trans. A*, **26A**(7):(1995) 1705. doi: 10.1007/BF02670757.

[7] A. P. Tsai, A. Niikura, *et al.*, *Philos Mag Lett*, **70**(3):(1994) 169. doi: 10.1080/09500839408240971.

[8] Y. Estrin, S. Arndt, *et al.*, *Acta Mater.*, **47**:(1999) 595. doi: 10.1016/S1359-6454(98)00362-0.

[9] J. Lépinoux, Y. Estrin, *J Physique IV*, **11**(PR4):(2001) 357.

[10] J. F. Nie, *Scr. Mat.*, **48**:(2003) 1009. doi: 10.1016/S1359-6462(02)00497-9.

[11] J. Lépinoux, Y. Estrin, *Acta Mater.*, **48**(17):(2000) 4337. doi: 10.1016/S1359-6454(00)00181-6.

[12] M. M. Avedesian, H. Baker, eds., *Magnesium and magnesium alloys*, 79, ASM specialty handbook, ASM, 1999.